Silicon (2022) 14:11001–11006
https://doi.org/10.1007/s12633-022-01836-y

ORIGINAL PAPER

Enhanced 2D Photonic Crystal Sensor for High Sensitivity Sulfuric Acid (H_2SO_4) and Hydrogen Peroxide (H_2O_2) Detection

Rami Zegadi[1] · Abdelouahab Zegadi[2] · Chemseddine Zebiri[1] · Said Mosbah[1] · Samira Mekki[1] · Mohamed Lamine Bouknia[1] · Hanane Bendjedi[1]

Received: 19 January 2022 / Accepted: 19 March 2022 / Published online: 30 March 2022

Abstract

In this study, an enhanced two-dimensional photonic crystal-based chemical sensor has been simulated to detect the concentrations of the two chemical substances sulfuric acid (H_2SO_4) and hydrogen peroxide (H_2O_2) using deionized water as a reference. The proposed structure is a ring resonator, consisting of circular silicon rods in air with a hexagonal array, and an overall size of 10 μm×11.5 μm in the X and Z directions, respectively. The simulated structure was proposed to have a consistent photonic band gap. The change in concentration affects the refractive index, which induces a shift in the resonance wavelength. The optical parameters are analyzed by the Finite Difference Time Domain method. The sensor performances, such as the sensitivity, the quality factor, the figure of merit, and the limit of detection were obtained and discussed. The results obtained are very promising and demonstrate the strong potential of the proposed sensor for chemical or biosensing applications. A maximum sensitivity of 1200 nm/RIU was achieved with the proposed sensor.

Keywords 2D photonic crystals · Sulfuric acid detection · Hydrogen peroxide detection · Sensitivity · Transmission

1 Introduction

The development of chemical and biological sensors has become a significant challenge to meet current needs in fields as varied as medicine (detection of pathogens) [1], agri-food (microbiological analyses) [2], and security (detection of toxic gases) [3], with increasingly high requirements. The real-time analysis must be favored, the response must be easy to read and extremely fast, the devices must be compact and can be incorporated into integrated or embedded electronic detection systems, and finally, the manufacturing cost must be reduced [2, 4–6]. These needs for more and more efficient detection have led to the emergence of new technological solutions to solve complex problems in radiofrequency fields [7], optoelectronics[8], and microwave detection [9]. Biophotonics is a research field with substantial potential for developing of generic transducers [10]. It is based on the use of optical techniques to study and characterize biological phenomena such as the interaction between two types of molecules (target and probe), a process which is one of the techniques used in biosensors [2, 10–12]. In parallel, the progress of nanotechnology, which allows to manipulate matter with a nanometric resolution, and thus at a scale adapted to the biomolecule, offers the possibility to develop new high performance detection platforms [10, 12–15]. Consequently, the growing demand for miniaturized devices for chemical and biological analysis systems has generated a strong interest in developing integrated optical systems on a chip [10, 16]. In this context, many structures based on integrated optics have been proposed. In particular, photonic crystals (PCs) exhibit excellent optical properties leading to the design of new photonic devices for applications in various industrial and high technology sectors, such as telecommunications (PC fibers), optoelectronics (lasers, photodetectors), and biodetection [10, 16–18]. Indeed, PCs constitute a platform of choice for such an application: the periodic nano structuring of the material allows ultimate control of the light in the spatial and temporal domains while being sensitive to the presence of the molecules to be detected [10, 16]. Three structures of photonic crystals are counted according to their geometry, namely 1D, 2D ,and 3D. The study focused on a 2D

✉ Rami Zegadi
ramizegadi@univ-setif.dz

[1] Department of Electronics, Faculty of Technology, LEPCI Laboratory, Ferhat Abbas University, Sétif 1, 19000 Sétif, Algeria

[2] Department of Physics, Faculty of Science, Ferhat Abbas University, Sétif 1, 19000 Sétif, Algeria

structure that allows light confinement and a wide photonic band gap [10].

H_2SO_4 and H_2O_2 are essential chemical substances in the industry [10, 19]. Sulfuric acid is one of the most important industrial chemicals [19]. Its applications are diverse in many areas of science and technology, including dissolution and processing of ores and minerals, resin manufactures, catalytic processes, accumulators, and fertilizer production [19]. Its range of acidity values meets the requirements of the industry [19, 20]. Due to its oily and corrosive nature and high density must be diluted to a specific concentration to obtain the desired results [19, 20]. Knowing its precise concentration is crucial. The other product studied is hydrogen peroxide. It is used as a bleaching agent in textiles, and mineral industries due to its oxidizing capabilities [21]. Waste water treatment removal of organic and inorganic contaminants are the most common applications [22].

In this paper, a two-dimensional photonic crystal-based resonator was simulated to detect the concentrations of the two chemicals H_2SO_4 and H_2O_2, taking deionized water as a reference. This sensor allows to determine the concentration of these two diluted products with precision.

2 Theory

2.1 Numerical Analysis

One fundamental property of photonic crystals is the photonic band gap. The structure of the latter can be described as an optical insulator. Since the transmission of electromagnetic waves in a specific range of frequencies is forbidden, there is no light propagation over a specific range of wavelengths. The propagation of light can be manipulated by creating a defect in the structure. The variation of the sample's in the resonator induces a shift in the resonance wavelength. The solution of the differential magnetic field equation derived from Maxwell's equations allows us to calculate the sensor parameters using the following equation [23].

$$\nabla \times \left(\frac{1}{\epsilon}\nabla \times H\right) = \left(\frac{\omega}{c}\right)^2 H \quad (1)$$

where H is the magnetic field and c is the speed of light. ε is the permittivity, ω is the resonant frequency and $\left(\frac{\omega}{c}\right)^2$ represent the eigenvalues. We notice that the dielectric function ε is inversely proportional to the frequency ω.

2.2 Proposed Structure

At the first step, it is necessary to define the structure that used for the detection. Figure 1 shows the simulated photonic crystal-based biosensor using a ring resonator. It consists of a hexagonal array of circular silicon rods placed in an air background. The number of rods in the X and Z directions is 21 and 21, respectively.

The proposed sensor consists of two optical waveguides: a bus waveguide and a dropping waveguide. The bus waveguide acts as an input port placed at one end, while the dropping waveguide acts as an output port at the other end. Both waveguides can be designed using bi-periodicity. Bi-periodicity is nothing more than reducing the radius of the waveguide rods with a radius of 50 nm compared to the rest of the structure with a radius of 105 nm. The resonator is the heart of the proposed biosensor, which is placed in the center. It is composed of two rings, the inner and outer rings. The radius of the inner and outer ring rods are both 105 nm. The central elliptical rod has an inner and outer radius of 150 nm and 105 nm, respectively. The distance between two rods is about 547 nm across the structure, and it is also called lattice constant denoted by a. The dielectric constant of the Si rod is 11.97 (refractive index = 3.46). The size of the sensor is about 11.5 μm×10 μm.

2.3 Detection Principle

When light propagates from the waveguide (input port) through the sensor resonator where the sample is deposited, molecular interactions due to the sample deposition induce a change in the refractive index. As a result, there is a shift in the resonance wavelength with variations in the transmitted power. The photodetector detects these variations (output port). Figure 2 shows the schematic representation of the detection mechanism, which consists of several elements such as the

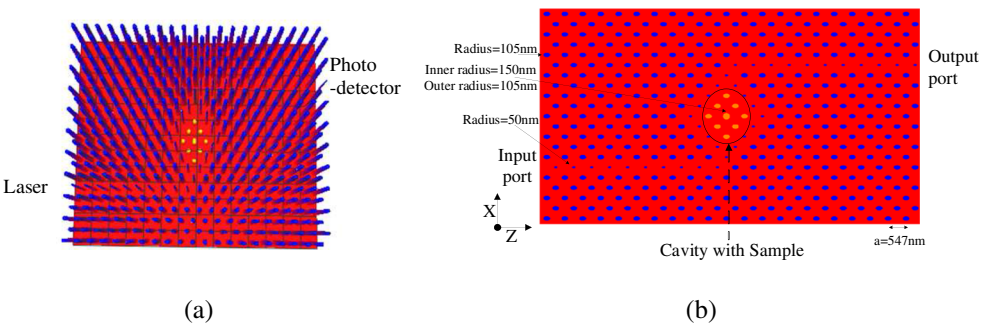

Fig. 1 Structure of the proposed chemical sensor: (**a**). Perspective view, (**b**). Front view

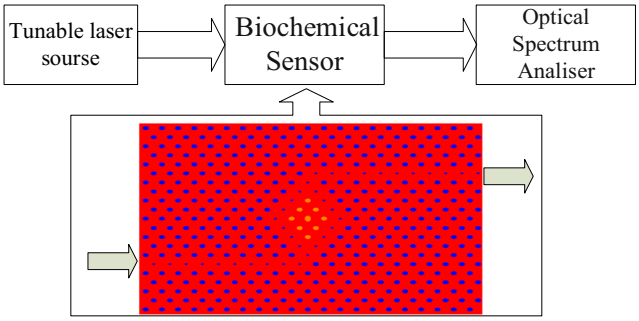

Fig. 2 Schematic representation of the detection mechanism

optical source, the biochemical sensor based on photonic crystals, the photodetector, the signal processing unit, and display.

3 Results and Discussions

3.1 Photonic Bandgap

The periodic structure does not allow a specific range of wavelengths which is called photonic band gap (PBG). The propagation of electromagnetic waves within the PBG region is prohibited. Figure 3 shows the photonic band gap of the proposed structure.

The PWE software is used to calculate the existing PBGs for different transverse electrical (TE) and magnetic (TM) polarizations. For the TE polarization, the main PBG is between the wavelengths 1149 and 1876 nm, corresponding to the third optical transmission window. The PBG for the TM mode, the narrow band is between the wavelengths 561 and 624 nm. The PBG for the TE mode is shown in Fig. 3(a), while Fig. 3(b) shows the one obtained for the TM mode.

The wavelength range of 1149 to 1876 nm is preferred because it belongs to the third communication window. The PBG in TE mode is considered for the sensor design. Figure 4 shows the electric field distribution of the resonator for the TE mode at a resonance wavelength of $\lambda_r = 1529$ nm .

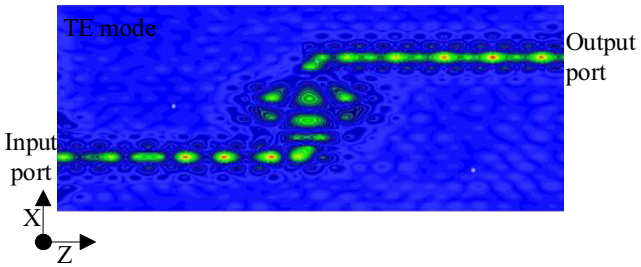

Fig. 4 The electric field distribution

3.2 Physical Properties of H_2O_2 and H_2SO_4

Sulfuric acid and hydrogen peroxide are the chemical substances investigated in this paper. The refractive indices of the two chemical substances, namely H_2O_2 and H_2SO_4, were obtained using the refractometer (ATAGO, Japan) at 18 °C [12]. In order to show the evolution of the refractive indices according to the two substances. There is a proportionality between the concentration and the refractive index values of H_2SO_4 and H_2O_2 is observed. The increase of one induces the other. It is noted that H_2SO_4 has a slightly higher refractive index than H_2O_2 [12]. Figure 5 shows the refractive index values for H_2SO_4 and H_2O_2 as a function of different concentration percentages that are used for the rest of the analysis.

3.3 Detection

The structure has been designed in such a way that a maximum of light transits through the cavity where the sample has been deposited. The variations caused by the refractive index of the samples in the transmission spectra are examined.

Figure 6 shows how the resonance wavelength is sensitive to the variation of the refractive index sample (1.33, 1.37, 1.41, and 1.42 RIU) corresponding to the H_2SO_4 concentrations (0%, 30%, 60%, and 90% respectively), placed in the central cavity. A transmission resonance spectra shift to the right (to longer wavelengths) is observed with an increasing

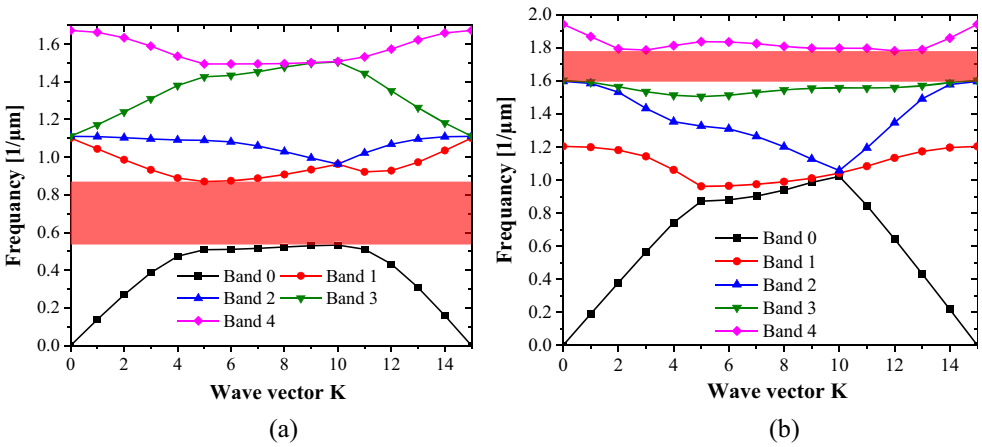

Fig. 3 (**a**) PBG for the transverse electric (TE) mode of the structure (**b**) PBG for the transverse magnetic (TM) mode

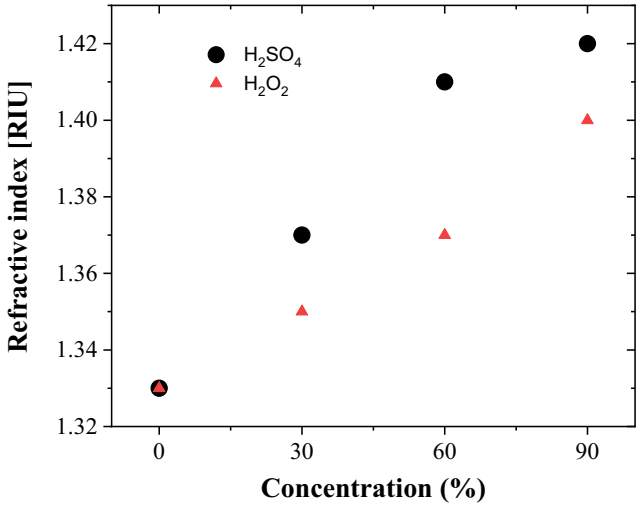

Fig. 5 Refractive index versus concentration of H_2SO_4 and H_2O_2 [12]

refractive index of H_2SO_4 (Fig. 6.a). Note that the refractive index n = 1.33 of deionized water is considered as a reference. The shift in the resonance wavelength is due to the variation of the refractive index accompanying different substance concentrations. Figure 6(b) shows that the resonance wavelength shift is close-fitting in linear shape versus the concentrations (wavelength = 0.77 + 0.57*RIU).

The transmitted light traveling through the sensor structure for different concentrations of H_2O_2 (0%, 30%, 60% and 90%) deposited in the center is shown in Fig. 7(a). These concentrations correspond to refractive indices (n) (1.33, 1.35, 1.37 and 1.4 RIU). The resonance wavelength shifts to the right with increasing sample concentration of H_2O_2.

Figure 7(b) shows the shift of the resonance wavelength for different concentrations of H_2O_2. The obtained curve has an exponential form (wavelength = 1.56–5.26 exp(-RIU/0.022). The refractive index n = 1.33 of deionized water is considered as a reference.

3.4 Analysis of Sensor Performance

The performance of a sensor is determined by many parameters of which the most important is the sensitivity whose equation is given by [10]:

$$S = \frac{\lambda}{\Delta n} \tag{2}$$

where Δλ is the difference in resonance wavelengths between each concentration of the chemical liquid (H_2SO_4 or H_2O_2) and the resonance of zero concentration (deionized water):

$$\lambda = \lambda_{C\%} - \lambda_{0\%} \tag{3}$$

Δn represents the change in the refractive index of the sample for different concentrations relative to the refractive index of deionized water.

Another parameter, as important as the previous one, is the quality factor Q which can be calculated according to the relation[10]:

$$Q = \frac{\lambda_r}{\Delta\lambda_{1/2}} \tag{4}$$

where λ_r is the resonant wavelength while $\Delta\lambda_{1/2}$ represents the full width at half maximum of the intensity.

The last two parameters calculated are the figure of merit (FOM) and the limit of detection (LOD) which are very useful. To calculate them the following two equations are used [10]:

$$FOM = \frac{SQ}{\lambda_r} \tag{5}$$

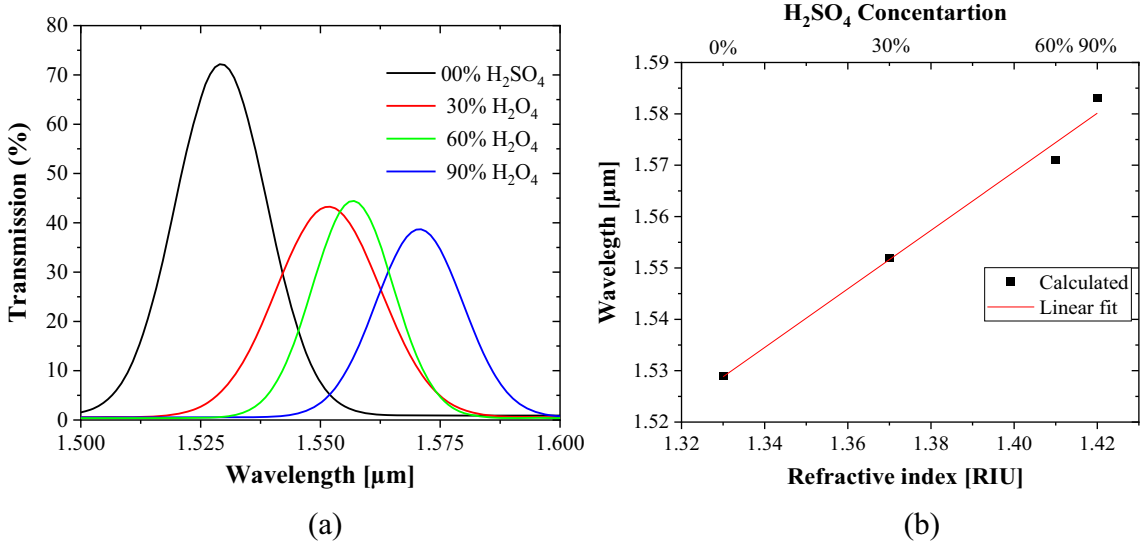

Fig. 6 (**a**) H_2SO_4 transmission spectra of the biochemical sensor designed for different concentrations. (**b**) The wavelength shift versus refractive indices

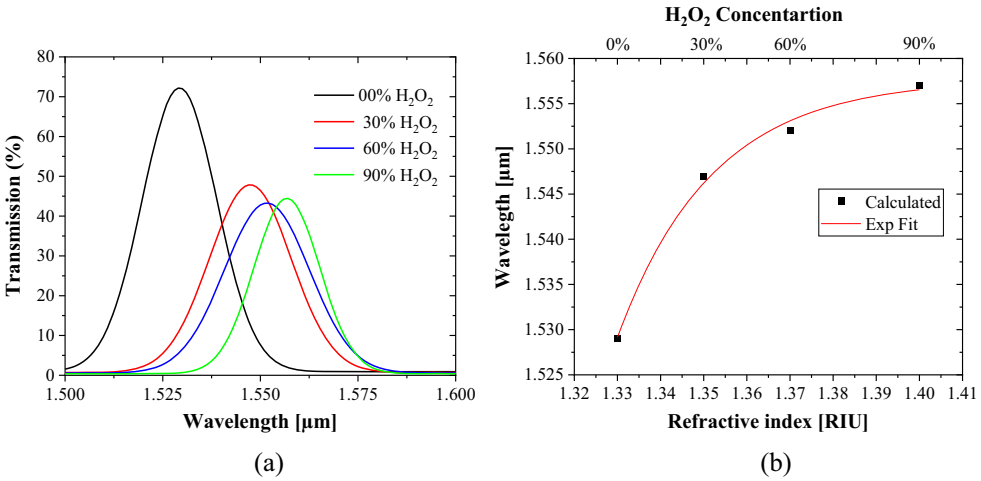

(a) (b)

Fig. 7 (**a**) H_2O_2 transmission spectra of the biochemical sensor designed for different concentrations. (**b**) The wavelength shift as a function of changing refractive indices

Table 1 Simulated sensor performance for different concentrations of H_2SO_4

Concentration H_2SO_4	RIU	λ_r [nm]	S [nm/RIU]	$\Delta\lambda_{1/2}$ [nm]	Q	FOM [RIU^{-1}]	LOD [RIU]
0%	1.33	1529	----------	22	70	--------	-----
30%	1.37	1552	575	26	60	22	$4.43\ 10^{-3}$
60%	1.41	1571	525	21	75	25	$4.00\ 10^{-3}$
90%	1.42	1583	600	27	59	22	$4.43\ 10^{-3}$

$$LOD = \frac{\lambda_r}{10SQ} \tag{6}$$

The resonance wavelength λ_r, sensitivity S, quality factor Q, figure of merit FOM, and detection limit are shown in Tables 1 and 2 for H_2SO_4 and H_2O_2, respectively.

As shown in Tables 1 and 2, the proposed sensor has very promising results. For sulfuric acid, a maximum sensitivity of 600 nm/RIU was achieved for a concentration of 90%. When the concentration is 60%, the sensitivity is 525 nm/RIU with a quality factor of 75, a FOM of about 25 RIU^{-1} for a detection limit of 4×10^{-3} RIU. If the sensitivity is calculated between the 60% and 90% concentrations, a sensitivity of 1200 nm/RIU is reached.

For hydrogen peroxide, a maximum sensitivity of 900 nm/RIU was reached for a concentration of 30% for a quality factor of 62, a FOM merit factor of about 36 RIU^{-1}, and a detection limit of 2.7×10^{-3} RIU.

In the literature, Balveer et al. obtained a sensitivity of 35 nm/RIU for H_2SO_4 and 9.4 for H_2O_2 [12]. Compared to other sensors works, Ching et al. achieved a sensitivity of 304 nm/ RIU [13], Gao et al. found a sensitivity of 656 nm/ RIU [14], and Francis et al. reached a sensitivity of 560 nm/RIU [15]. The sensor proposed in this paper shows very competitive results.

4 Conclusions

A two-dimensional photonic crystal-based chemical sensor has been simulated to detect sulfuric acid and hydrogen peroxide concentrations. The simulated sensor consists of a

Table 2 Simulated sensor performance for different H_2O_2 concentrations

Concentration H_2O_2	RIU	λ_r [nm]	S [nm/RIU]	$\Delta\lambda_{1/2}$ [nm]	Q	FOM [RIU^{-1}]	LOD [RIU]
0%	1.33	1529	----------	22	70	-------	-------
30%	1.35	1547	900	25	62	36	$2.7\ 10^{-3}$
60%	1.37	1552	575	26	60	22	$4.5\ 10^{-3}$
90%	1.40	1557	400	19	82	21	$4.7\ 10^{-3}$

hexagonal array of silicon rods in the air. Knowing the refractive indices of the different concentration substances, the sensitivity, the quality factor, the figure of merit, and the limit of detection were obtained. An improved maximum sensitivity of 1200 nm/RIU and 900 was reached for H_2SO_4 and H_2O_2, respectively. The simulated sensor is very sensitive to low refractive index variation, which is efficient. It can measure the concentrations of both chemicals with high accuracy.

Author Contributions R.Z. carried out the simulations, wrote the paper, and prepared the original draft. R.Z., A.Z., C.Z., S.M., S.M., M.L.B., H.B. contributed to the organization of the paper, writing, and proofreading. All authors have read and agreed to the published version of the manuscript.

Funding This work was supported by the Algerian ministry of higher education and scientific research.

Data Availability Not applicable.

Code Availability The data presented in this study are available on request from the corresponding author.

Declarations

Ethics Approval Not applicable.

Consent to Participate Not applicable.

Consent for Publication Not applicable.

Conflict of Interest The authors declare no competing interests.

References

1. Hossain MdS, Sen S (2021) Design and performance improvement of optical chemical sensor based Photonic Crystal Fiber (PCF) in the Terahertz (THz) wave propagation. Silicon 13:3879–3887. https://doi.org/10.1007/s12633-020-00696-8
2. Maddela NR, Chakraborty S, Prasad R (2021) Nanotechnology for advances in medical microbiology. Springer Nature, Berlin
3. Zegadi R, Lorrain N, Bodiou L et al (2021) Enhanced mid-infrared gas absorption spectroscopic detection using chalcogenide or porous germanium waveguides. J Opt 23:035102. https://doi.org/10.1088/2040-8986/abdf69
4. Singh NA, Kumar P (2021) Nanosensors applications in food, medicine, agriculture and nanotoxicology. In: Kumar V, Guleria P, Ranjan S et al (eds) Nanotoxicology and Nanoecotoxicology, vol 2. Springer International Publishing, Cham, pp 1–24
5. Sundar DS, Umamaheswari C, Sridarshini T et al (2019) Compact four-port circulator based on 2D photonic crystals with a 90° rotation of the light wave for photonic integrated circuits applications. Laser Phys 29:066201. https://doi.org/10.1088/1555-6611/ab1413
6. Zhang R, Wang Q, Zheng X (2018) Flexible mechanochromic photonic crystals: routes to visual sensors and their mechanical properties. J Mater Chem C 6:3182–3199. https://doi.org/10.1039/C8TC00202A
7. Amphawan A, Chaudhary S, Neo T-K et al (2021) Radio-over-free space optical space division multiplexing system using 3-core photonic crystal fiber mode group multiplexers. Wirel Netw 27:211–225. https://doi.org/10.1007/s11276-020-02447-4
8. Zegadi R, Lorrain N, Meziani S et al (2022) Theoretical demonstration of the interest of using porous germanium to fabricate multilayer vertical optical structures for the detection of SF6 gas in the mid-infrared. Sensors 22:844. https://doi.org/10.3390/s22030844
9. Kumar N, Kaliramna S, Singh M (2021) Design of cold plasma based ternary photonic crystal for microwave applications. Silicon. https://doi.org/10.1007/s12633-021-01405-9
10. Parandin F, Heidari F, Rahimi Z, Olyaee S (2021) Two-dimensional photonic crystal biosensors: a review. Opt Laser Technol 144:107397. https://doi.org/10.1016/j.optlastec.2021.107397
11. Fathi F, Rashidi M-R, Pakchin PS et al (2021) Photonic crystal based biosensors: Emerging inverse opals for biomarker detection. Talanta 221:121615. https://doi.org/10.1016/j.talanta.2020.121615
12. Painam B, Kaler RS, Kumar M (2017) Photonic crystal waveguide biochemical sensor for the approximation of chemical components concentrations. Plasmonics 12:899–904. https://doi.org/10.1007/s11468-016-0341-z
13. Qi C, Shutao W, Jiangtao L et al (2020) Refractive index sensor based on photonic crystal nanocavity. Opt Commun 464:125393. https://doi.org/10.1016/j.optcom.2020.125393
14. Gao Y, Dong P, Shi Y, Shi Y (2020) Suspended slotted photonic crystal cavities for high-sensitivity refractive index sensing. Opt Express OE 28:12272–12278. https://doi.org/10.1364/OE.386678
15. Segovia-Chaves F, Trujillo Yague JC (2021) Sensitivity optimization of cells immersed in a cavity surrounded by thin graphene layers in one-dimensional photonic crystals. Optik 231:166355. https://doi.org/10.1016/j.ijleo.2021.166355
16. Shastri BJ, Tait AN, Ferreira de Lima T et al (2021) Photonics for artificial intelligence and neuromorphic computing. Nat Photonics 15:102–114. https://doi.org/10.1038/s41566-020-00754-y
17. Zegadi R, Ziet L, Zegadi A (2020) Design of high sensitive temperature sensor based on two-dimensional photonic crystal. Silicon 12:2133–2139. https://doi.org/10.1007/s12633-019-00303-5
18. Zegadi R, Ziet L, Satour FZ, Zegadi A (2019) Design of a wide ranging highly sensitive pressure sensor based on two-dimensional photonic crystals. Plasmonics 14:907–913. https://doi.org/10.1007/s11468-018-0873-5
19. Wang H, Du H, Liu K et al (2021) Sustainable preparation of bifunctional cellulose nanocrystals via mixed H2SO4/formic acid hydrolysis. Carbohydr Polym 266:118107. https://doi.org/10.1016/j.carbpol.2021.118107
20. Gao Q, Sun Q, Zhang P et al (2021) Sulfuric acid decomposition in the iodine–Sulfur cycle using heat from a very high temperature gas-cooled reactor. Int J Hydrog Energy 46:28969–28979. https://doi.org/10.1016/j.ijhydene.2020.08.074
21. Gharibi H, Mehaney A (2021) Two-dimensional phononic crystal sensor for volumetric detection of hydrogen peroxide (H2O2) in liquids. Phys E 126:114429. https://doi.org/10.1016/j.physe.2020.114429
22. Talaiekhozani A, Rezania S, Kim K-H et al (2021) Recent advances in photocatalytic removal of organic and inorganic pollutants in air. J Clean Prod 278:123895. https://doi.org/10.1016/j.jclepro.2020.123895
23. Cho S, Takahashi M, Fukuda J et al (2021) Directed self-assembly of soft 3D photonic crystals for holograms with omnidirectional circular-polarization selectivity. Commun Mater 2:1–9. https://doi.org/10.1038/s43246-021-00146-x